BJP British Journal of Pharmacology

DOI:10.1111/bph.12868
www.brjpharmacol.org

RESEARCH PAPER

Dopamine D_1 and corticotrophin-releasing hormone type-2α receptors assemble into functionally interacting complexes in living cells

J Fuenzalida[1,*], P Galaz[1,*], K A Araya[1,†], P G Slater[1], E H Blanco[1], J M Campusano[1], F Ciruela[2] and K Gysling[1]

[1]*Millennium Nucleus in Stress and Addiction, Department of Cellular and Molecular Biology, Faculty of Biological Sciences, Pontificia Universidad Católica de Chile, Santiago, Chile, and* [2]*Unitat de Farmacologia, Facultat de Medicina, Departament de Patologia i Terapèutica Experimental, IDIBELL, L'Hospitalet de Llobregat, Universitat de Barcelona, Barcelona, Spain*

Correspondence
Dr Katia Gysling, Alameda 340, Santiago 8331150, Chile. E-mail: kgysling@bio.puc.cl
Dr Francisco Ciruela, Av. Feixa Llarga, s/n, L'Hospitalet del Llobregat, Barcelona 08907, Spain. E-mail: fciruela@ub.edu

*Both authors contributed equally to this work.

†Present address: Facultad de Ciencias, Universidad San Sebastian, Puerto Montt, Chile.

Received
24 February 2014
Revised
5 July 2014
Accepted
23 July 2014

BACKGROUND AND PURPOSE

Dopamine and corticotrophin-releasing hormone (CRH; also known as corticotrophin-releasing factor) are key neurotransmitters in the interaction between stress and addiction. Repeated treatment with cocaine potentiates glutamatergic transmission in the rat basolateral amygdala/cortex pathway through a synergistic action of D_1-like dopamine receptors and CRH type-2α receptors ($CRF_{2\alpha}$ receptors). We hypothesized that this observed synergism could be instrumented by heteromers containing the dopamine D_1 receptor and $CRF_{2\alpha}$ receptor.

EXPERIMENTAL APPROACH

$D_1/CRF_{2\alpha}$ receptor heteromerization was demonstrated in HEK293T cells using co-immunoprecipitation, BRET and FRET assays, and by using the heteromer mobilization strategy. The ability of D_1 receptors to signal through calcium, when singly expressed or co-expressed with $CRF_{2\alpha}$ receptors, was evaluated by the calcium mobilization assay.

KEY RESULTS

$D_1/CRF_{2\alpha}$ receptor heteromers were observed in HEK293T cells. When singly expressed, D_1 receptors were mostly located at the cell surface whereas $CRF_{2\alpha}$ receptors accumulated intracellularly. Interestingly, co-expression of both receptors promoted D_1 receptor intracellular and $CRF_{2\alpha}$ receptor cell surface targeting. The heteromerization of $D_1/CRF_{2\alpha}$ receptors maintained the signalling through cAMP of both receptors but switched D_1 receptor signalling properties, as the heteromeric D_1 receptor was able to mobilize intracellular calcium upon stimulation with a D_1 receptor agonist.

CONCLUSIONS AND IMPLICATIONS

D_1 and $CRF_{2\alpha}$ receptors are capable of heterodimerization in living cells. $D_1/CRF_{2\alpha}$ receptor heteromerization might account, at least in part, for the complex physiological interactions established between dopamine and CRH in normal and pathological conditions such as addiction, representing a new potential pharmacological target.

Abbreviations

CFP, cyan fluorescent protein; CRH, corticotrophin-releasing hormone; $CRF_{2\alpha}$ receptor, corticotrophin-releasing hormone type-2_α receptor; YFP, yellow fluorescent protein

Table of Links

TARGETS	LIGANDS
5-$HT_{2A/C}$ receptor	cAMP
α_{1B}-adrenoceptor	CRH (CRF)
μ opioid receptor	Dopamine
CB_1 receptor	Glutamate
CRF_1 receptor	SCH23390
CRF_2 receptor	Urocortin 1
D_1 receptor	
D_2 receptor	
$GABA_{B2}$ receptor	

This Table lists key protein targets and ligands in this document, which are hyperlinked to corresponding entries in http://www.guidetopharmacology.org, the common portal for data from the IUPHAR/BPS Guide to PHARMACOLOGY (Pawson *et al.*, 2014) and are permanently archived in the Concise Guide to PHARMACOLOGY 2013/14 (Alexander *et al.*, 2013b).

Introduction

Stress-induced relapse to drug seeking is one of the main problems in drug addiction treatment (Koob, 2008), in part because of the lack of suitable pharmacological targets. It has been shown that the exposure to drugs of abuse and to stressful stimuli induce similar neuronal plastic changes strengthening excitatory inputs to midbrain dopaminergic neurons (Saal *et al.*, 2003). However, the mechanisms of this interaction are still not fully understood. The available evidence supports a key role for the neurotransmitters corticotrophin-releasing hormone (CRH also known as corticotrophin-releasing factor) and dopamine driving the interaction between stress and addiction (Corominas *et al.*, 2010; George *et al.*, 2012; Gysling, 2012; Zorrilla *et al.*, 2014). CRH signalling occurs through the activation of two class B1 GPRC (Alexander *et al.*, 2013), CRF_1 and CRF_2 receptors. Several studies have shown that the CRF_1 receptor has a key role in plastic changes associated with stress and addiction (Shalev *et al.*, 2010). However, more recently, the role of the CRF_2 receptor in plastic changes induced by addictive drugs has also been recognized (Wang *et al.*, 2007; Hahn *et al.*, 2009; Cadet *et al.*, 2014; Guan *et al.*, 2014). Wise and his group (Wang *et al.*, 2005) have shown that a stressful stimulus induces the release of CRH in the ventral tegmental area (VTA) of both naive and cocaine-experienced rats, and that glutamate release becomes sensitized to CRH only in cocaine-experienced rats. They have shown that this sensitization of VTA glutamate is mediated by CRF_2 receptors (Wang *et al.*, 2007). In addition, Orozco-Cabal *et al.* (2008), using an electrophysiological approach, showed a synergism between D_1-like dopamine receptors and CRF_2 receptors in basolateral amygdala to medial prefrontal cortex synaptic transmission in rats subjected to repeated cocaine treatment. Thus, the receptors involved in this synergism could be, in part, responsible for the link between addiction and stress.

Increasing evidence shows that the ability of GPCRs to form oligomers plays a key role in synaptic transmission (Ciruela *et al.*, 2012). It has been documented that dopamine receptors are able to form heteromers between them and with other GPCRs (Perreault *et al.*, 2014). Interestingly, it has been shown that the heteromerization of D_1 and D_2 dopamine receptors, a novel receptorial entity able to induce calcium mobilization through a switch to Gq-mediated activation of PLC (Lee *et al.*, 2004; Rashid *et al.*, 2007). More recent evidence suggests that the mechanisms of calcium mobilization induced by the heteromerization of D_1 and D_2 receptors are more complex, implying other intracellular mediators (Chun *et al.*,).

The possible heteromerization between D_1 and CRF_2 receptors could be responsible for the synergism between dopamine and CRH transmission (Orozco-Cabal *et al.*, 2008). As the α-isoform of CRF_2 receptors is the main isoform expressed in the brain (Chalmers *et al.*, 1995; Lovenberg *et al.*, 1995; Dautzenberg and Hauger, 2002), we hypothesized that D_1 and $CRF_{2\alpha}$ receptors assemble into functional interacting complexes (i.e. heteromers). The existence of a $D_1/CRF_{2\alpha}$ receptor heteromer would constitute a novel potential target for drug addiction pharmacotherapy.

The present study aimed to determine the molecular and functional interactions between D_1 and $CRF_{2\alpha}$ receptors in living cells. Overall, we provide evidence of the existence of a novel and genuine $D_1/CRF_{2\alpha}$ receptor heteromer that behaves as a different receptorial entity to their individual constituents.

Methods

Plasmid constructs

The constructs encoding human D_1, CRF_1 and $CRF_{2\alpha}$ receptors were isolated by Touch-Down PCR using PfuUltra II Fusion HS DNA Polymerase (Agilent Technologies, Palo Alto, CA, USA). PCR products were digested with the respective restriction enzymes and cloned into the expression vector listed in Table 1. The D_2 $receptor^{YFP}$ and $GABA_{B2}$ $receptor^{YFP}$ constructs

Table 1

Constructs information

Construct	Vector	Restriction enzyme	Primers
D_1 receptor	pcDNA 3.1	EcoRV and NotI	CCGGATATCGGCGCCAACATGAGGACTCTGAACACC CGAGCGGCCGCTCAGGTTGGGTGCTGACCGTT
$CRF_{2\alpha}$ receptor	pcDNA 3.1	HindIII and XhoI	CCGAAGCTTGGCGCCACCATGGACGCGGCACTGCTC CGACTCGAGTCACACAGCGGCCGTCTGCTT
D_1 receptor^{YFP}	pEYFP-N1	EcoRI and BamHI	CTCGAATTCGCCACCATGAGGACTCTGAACACC CGTCGCCGTCCAGCTCGACCAG
$CRF_{2\alpha}$ receptor^{CFP}	pECFP-N1	EcoRI and KpnI	CCGGAATTCGCCACCATGGACGCGGCACTG CGTCGCCGTCCAGCTCGACCAG
CRF_1 receptor^{YFP}	pEYFP-N1	EcoRI and KpnI	GTGGAATTCACCATGGGAGGGCAC CCGCGGTACCCAGACTGCTGTGGA
D_1 receptor$^{myc/His}$	pcDNA 3.1 myc/His	EcoRV and BamHI	CCGGATATCGGCGCCAACATGAGGACTCTGAACACC CGAGGATCCGGTTGGGTGCTGACCGTT
$CRF_{2\alpha}$ receptor^{Rluc}	pRluc-N1	EcoRI and KpnI	CTCGAATTCGCCACCATGGACGCGGCACTGCTC CGCGGTACCGCCACAGCGGCCGTCTGCTTG
D_1 receptor-NLS^{YFP}	pEYFP-N1	EcoRI and BamHI	CTCGAATTCGCCACCATGAGGACTCTGAACACC CCTAAGAGGGTTGAAAATCTTTTAAATTTTTTAGCATTAAAGGCATAAATG GCCTTTAATGCTAAAAAATTTAAAAGATTTTCAACCCTCTTAGGATGC CGTCGCCGTCCAGCTCGACCAG
$CRF_{2\alpha}$ receptor^{Flag}	pcDNA 3.1	HindIII and NotI	CCGAAGCTTGGCGCCACCATGGACGCGGCACTGCTC GTCGTCATCCTTGTAGTCCACAGCGGCCGTCTGCTT GACTACAAGGATGACGACGATAAGTGAGCG GAATAGAATGACACCTACTCAGACAATCGC

Each construct was generated by PCR amplification and the primers used are listed. The restriction enzymes and vectors into which they were sub-cloned are also indicated.

were prepared as previously described (Canals *et al.*, 2003). The $CRF_{2\alpha}$ receptor^{Flag} and D_1 receptor-nuclear localization sequence (NLS)^{YFP} were generated by PCR overlapping extension as previously described (Heckman and Pease, 2007), using two coupled primers each. The primers used are listed in Table 1 and the restriction sites within the primers are underlined. All constructs were confirmed by DNA sequencing.

Cell culture and transfection

HEK293T cells were grown in 100 mm plates with DMEM (Gibco, Gaithersburg, MD, USA) supplemented with 10% FBS (Hyclone Labs, Logan, UT, USA), 1% penicillin/streptomycin 100× (Gibco), 2 mM GlutaMax (Gibco) and 1% non-essential amino acids 100× (Gibco) at 37°C in a 5% CO_2 humidified atmosphere. Transfection was performed 24 h post seeding, using either Lipofectamine 2000 reagent (Invitrogen, Carlsbad, CA, USA) or linear polyethylenimine (Poly Sciences, Inc., Warrington, PA, USA).

Immunofluorescence

HEK293T cells (7×10^5) were grown on 24-well plates on coverslips coated with poly-L-lysine (Sigma, Saint Louis, MO, USA). Between 0.4 and 0.5 μg of plasmid DNA was transfected. Forty-eight hours post-transfection, the cells were fixed with 4% paraformaldehyde (PFA). In some cases, cells transfected with fluorescent chimeras were incubated for 10 min at room temperature with 5 μg mL^{-1} of WGA^{647} (Invitrogen) in PBS (Winkler Ltda., Santiago, Chile), washed and mounted with Dako mounting media (Dako, Carpenteria, CA, USA).

For immunodetection of wild-type receptors, cells were washed and permeabilized with 0.2% Triton-X100 (Sigma) for 10 min at room temperature, washed twice and blocked with PBS containing 1% BSA (Rockland Immunochemical, Gilbertsville, PA, USA) for 1 h at room temperature. Cells were incubated for 1 h at room temperature with primary antibodies: goat anti-CRF_2 receptor (dilution 1:200; sc-1826, Santa Cruz Biotechnology, Inc., Santa Cruz, CA, USA) and rabbit anti-D_1 receptor (dilution 1:200; sc-14001, Santa Cruz Biotechnology, Inc.) in PBS–BSA solution. Then, cells were washed and incubated for 1 h with the following secondary antibodies: donkey anti-goat $AlexaFluor^{488}$ and donkey anti-rabbit $AlexaFluor^{546}$. Cells were washed and mounted with mounting media (Dako). In the case of immunofluorescence for D_1 receptor$^{myc/His}$, a rabbit anti-mouse antibody was used (dilution 1:200; ab18185, Abcam, Cambridge, MA, USA). For calnexin, a rabbit anti-calnexin was used (dilution 1:200, Sigma).

Confocal microscopy

Fluorescence images were captured with a confocal microscope (Fluoview 1000, Olympus, New York, NY, USA) and Fluoview v6.0 software (Olympus). The images were digitally obtained with a 100× objective (N.A 1.4 oil) and using a sequential mode of laser scanning. All the images were obtained without Gain and with Offset Zero. Captured images were processed with ImageJ software (Rasband, WS, ImageJ, NIH, http://rsbweb.nih.gov/ij/). The deconvolution analysis was performed as previously described (Blanco *et al.*, 2011) with 'Iterative Deconvolve' plugins. The co-localization analysis was made with 'JaCoP' plugins. Pearson's coefficient was used to measure the overlap of the pixels in dual-channel images, reflecting the degree of dependency between two variables or fluorescent labels (Bolte and Cordelieres, 2006).

cAMP measurement

HEK293T cells (2×10^6) were grown in 60 mm plates and transiently transfected with 2 μg of DNA. Forty-eight hours post-transfection, cells were rapidly washed twice in HBSS (14065-056, Gibco), detached and resuspended in the same buffer with 100 μM IBMX (Sigma). Four thousand cells per well were stimulated with SKF83959 (Tocris Bioscience, Ellisville, MO, USA) or urocortin I (Sigma) prepared in HBSS supplemented with 100 μM IBMX, 5 mM HEPES and 2% DMSO or 100 μM IBMX, 5 mM HEPES and 0.1% BSA respectively. cAMP measurement were performed on 384-well plate using a homogenous time-resolved fluorescence (HTRF) cAMP dynamic 2 Kit (Cisbio International, Bagnols-sur-Cèze, France), according to the manufacturer's recommendations.

Protein extraction and immunoprecipitation

HEK293T (8×10^6) cells growing in a 100 mm dish were transiently transfected with D_1 receptor$^{myc/His}$, $CRF_{2\alpha}$ receptor^{Flag}, D_1 receptor$^{myc/His}$ plus $CRF_{2\alpha}$ receptor^{Flag} and pcDNA3.1 using Lipofectamine 2000 (Invitrogen). Protein extracts were obtained by using the modified protocol of Burgueño *et al.* (2003). In brief, 48 h post-transfection, the cells were collected in PBS and washed twice with PBS. Then, the cells were resuspended in lysis buffer (50 mM Tris-HCl, pH 8.0, 150 mM NaCl, 1 mM EDTA) with protease inhibitors Complete Mini (Roche Diagnostics, Indianapolis, IN, USA), incubated for 20 min on ice and centrifuged at 19 500× *g* for 30 min at 4°C. The pellet was resuspended in RIPA (50 mM Tris-HCl, pH 7.4, 150 mM NaCl, 0.25% deoxycholate, 1% NP-40, 1 mM EDTA, Millipore, Temecula, CA, USA) containing protease inhibitors, and homogenized through a piston sonicator (Cell Ultrasonic Disrrupter, Kontes, Vineland, NJ, USA) with two pulses of 5–10 s and then stood for 30 min on ice. Finally, the homogenate was centrifuged at 19 500× *g* for 30 min at 4°C. The soluble-rich membrane extracts were collected and the protein concentration determined with the Micro BCA™ Protein Assay Kit (Thermo Scientific, Rockford, IL, USA).

For inmunoprecipitation, the soluble-rich membrane extracts were pre-cleared with 'TrueBlot Anti-Rabbit Ig IP Beads' (eBioscience, San Diego, CA, USA). The samples were incubated with 0.8 μg rabbit anti-myc antibody (Ab9106, Abcam) according to the manufacturer's recommendations. Loading buffer 2× (8 M urea, 2% SDS, 100 mM DTT, 375 mM Tris, pH 6.8) was added to each sample. Immune complexes were dissociated by addition of DTT (to 25 mM) and heating to 37°C for 2 h and resolved by 8% SDS-PAGE with 8% urea. Proteins were transferred to nitrocellulose membranes and immunoblotted with mouse anti-Flag antibody (Stratagene, La Jolla, CA, USA), and then HRP-conjugated donkey anti-mouse IgG (dilution 1:5000, Jackson ImmnunoResearch Laboratories, Inc., West Grove, PA, USA). The immunoreactive bands were developed using a chemiluminescent detection kit ('SuperSignal West Pico Chemiluminescent Substrate', Thermo Scientific) according to the manufacturer's recommendations.

BRET assays

For BRET experiments, HEK293T cells transiently transfected with a constant amount (1 μg) of plasmid encoding $CRF_{2\alpha}$ receptor^{Rluc} and increasing amounts (0.25–3 μg) of plasmids encoding for D_1 receptor^{YFP}, D_2 receptor^{YFP} or $GABA_{B2}$ receptor^{YFP}, were rapidly washed twice in HBSS (137 mM NaCl, 5.4 mM KCl, 0.3 mM Na_2HPO_4, 0.4 mM KH_2PO_4, 4.2 mM $NaHCO_3$, 1.3 mM $CaCl_2$, 0.5 mM $MgCl_2$, 0.6 mM $MgSO_4$, 5.6 mM glucose, pH 7.4) containing 10 mM glucose, detached and resuspended in the same buffer. To control the cell number, protein concentration was determined using Micro BCA™ Protein Assay Kit (Thermo Scientific). Cell suspensions (20 μg protein) were distributed in triplicate into 96-well, black microplates with a clear bottom (Corning 3651, Corning, Stockholm, Sweden) for fluorescence measurement or white plates with a solid bottom (Corning 3600, Corning) for BRET determination. For BRET measurement, benzyl-coelenterazine (NanoLight Technology, Pinetop, AZ, USA) was added at a final concentration of 5 μM, and readings were performed 1 min after using the POLARstar Optima plate-reader (BMG Labtech, Durham, NC, USA) that allows the simultaneous integration of the signals detected with two filter settings (475 ± 30 and 535 ± 30 nm). The BRET ratio was defined as previously described (Canals *et al.*, 2003; Ciruela *et al.*, 2004). In brief, the BRET signal was determined by calculating the ratio of the light emitted by yellow fluorescent protein (YFP) (510–560 nm) over the light emitted by *R*luc (440–500 nm). The net BRET values were obtained by subtracting the BRET background signal detected when the *R*luc-tagged construct was expressed alone. Curves were fitted using a non-linear regression and one-phase exponential association fit equation using the GraphPad Prism software (GraphPad Prism, San Diego, CA, USA).

FRET experiments

FRET between $CRF_{2\alpha}$ receptor^{CFP} and D_1 receptor^{YFP} in living cells was determined by donor recovery after acceptor photobleaching. If FRET occurs, then the bleaching of the acceptor (i.e. YFP) yields a significant increase in fluorescence of the donor [i.e. cyan fluorescent protein (CFP)] (Vilardaga *et al.*, 2008). In brief, cells expressing CFP plus D_1 receptor^{YFP}, YFP plus $CRF_{2\alpha}$ receptor^{CFP}, $CRF_{2\alpha}$ receptor^{CFP} alone, $CRF_{2\alpha}$ receptor^{CFP} plus D_1 receptor^{YFP} or $CRF_{2\alpha}$ receptor^{CFP} plus D_2 receptor^{YFP} were mounted in an Attofluor holder (Warner Instruments, Hamden, CT, USA) and placed on an inverted Axio Observer microscope (Zeiss Microimaging, Oberkochen, Germany) equipped with a 63× oil immersion objective and a dual-emission photometry system (TILL Photonics,

Gräfelfing, Germany). A Polychrome V (Till Photonics) was used as the light source and signals detected by photodiodes were digitized using a Digidata 1440A analogue/digital converter (Molecular Devices, Sunnyvale, CA, USA). pCLAMP (Molecular Devices) and GraphPad Prism software were used for data collection and analysis respectively. Therefore, upon excitation at 436 ± 10 nm [beam splitter dichroic long-pass (DCLP) 460 nm] and an illumination time set to 10 ms at 10 Hz, the emission light intensities were determined at 535 ± 15 nm (YFP) and 480 ± 20 nm (CFP_{pre}) with a beam splitter DCLP of 505 nm. Subsequently, acceptor photobleaching was performed by direct illumination of YFP at 500 nm for 10 min. Finally, the emission intensities of YFP and CFP (CFP_{post}) were recorded again. FRET efficiency was calculated according to the equation: $FRET_{efficiency} = 1 - (CFP_{pre}/CFP_{post})$.

Calcium measurement

D_1 receptors alone or combined with $CRF_{2\alpha}$ receptors were transfected into HEK293T cells. Forty-eight hours after transfection, cells were loaded with 5 μM FURA-2 AM (Invitrogen) and 5 μM pluronic acid in HBSS (120 mM NaCl, 5.4 mM KCl, 0.8 mM $MgCl_2$, 15 mM glucose, 20 mM HEPES, pH 7.4) plus 1.8 mM $CaCl_2$ for 45 min at 37°C. Then, the medium was changed and allowed to de-esterify for 30 min at 37°C. Finally, the medium was changed to HCSS without calcium and fluorescence of FURA-2 AM was measured at 340 and 380 nm in a Spinning Disk confocal microscope (Olympus) (Leyton *et al.*, 2014).

Statistical analysis

Results are presented as means ± SEM and analyses were carried out with GraphPad Prism v5.0 (GraphPad Software). Accordingly, Mann–Whitney test or one-way ANOVA followed by Bonferroni *post hoc* test was used to determine significance.

Materials

SKF83959 [6-chloro-2,3,4,5-tetrahydro-3-methyl-1-(3-methylphenyl)-1H-3-benzazepine-7,8-diol hydrobomide] and SCH23390 [(R)-(+)-7-chloro-8-hydroxy-3-methyl-1-phenyl-2,3,4,5-tetrahydro-1H-3-benzazepine hydrochloride] were purchased from Tocris Biosciences (Bristol, UK). Urocortin I was purchased from Phoenix Peptides (Burlingame, CA, USA).

Results

Differential subcellular distribution of D_1 and $CRF_{2\alpha}$ receptors

The subcellular distribution of D_1 and $CRF_{2\alpha}$ receptors was evaluated. Accordingly, HEK293T cells were transiently transfected with D_1 or $CRF_{2\alpha}$ receptors tagged at their C-terminus with YFP and CFP (D_1 $receptor^{YFP}$ and $CRF_{2\alpha}$ $receptor^{CFP}$) respectively. The fluorescence labelling of the individual cells was classified into surface (bright ring surrounding the cell) or intracellular (dense intracellular fluorescence) as previously done for $\alpha_{1A/B}$- and α_{1D}-adrenoceptors respectively (Hague *et al.*, 2004b).

As shown in Figure 1A (upper), D_1 $receptor^{YFP}$ presented a mainly surface phenotype such as previously reported (O'Dowd *et al.*, 2005). Quantitative analysis indicated that 77.4 ± 2.8% of the cells presented the surface phenotype. In contrast, $CRF_{2\alpha}$ $receptor^{CFP}$ presented an intracellular phenotype (Figure 1A, bottom). Quantitative analysis indicated that 85.3 ± 2.7% of cells presented an intracellular phenotype. To remove the influence of the tagged fluorescence proteins in the subcellular distribution pattern of these receptors, immunofluorescence was performed in HEK293T cells transiently transfected with D_1 or $CRF_{2\alpha}$ receptors. As shown in Figure 1B, wild-type receptors showed the same phenotype as tagged receptors.

It has been reported that both D_1 and $CRF_{2\alpha}$ receptors signal through $G_{\alpha s}$ in HEK293T cells, increasing cAMP levels (Dautzenberg and Hauger, 2002; Neve *et al.*, 2004; Gutknecht *et al.*, 2008). In order to determine if the transfected receptors were functional in the conditions of the present study, we measured cAMP levels induced by respective agonists in HEK293 cells transfected with each receptor alone. We used the HTRF technique to measure cAMP levels induced by the presence of increasing concentrations of SKF83959, D_1R agonist and of urocortin I, a CRH_2R agonist. The concentration–response curves showed that activation of both receptors induced cAMP accumulation in a ligand concentration-dependent manner with a $Log(EC_{50}) = -9.122 \pm 0.15$ for SKF83959 (Fig. 1C) and $Log(EC_{50}) = -10.11 \pm 0.29$ for urocortin I (Figure 1D). To discount the possibility that cAMP accumulation is due to the activation of endogenous GPCRs present in HEK293T cells, we tested the effect of each ligand on HEK293T cells transfected only with the empty vector.

D_1 and $CRF_{2\alpha}$ receptors mutually modify their subcellular distribution

It has been reported that receptor heteromerization could change the dynamics and subcellular localization of the receptors involved (Terrillon and Bouvier, 2004). Thus, we evaluated the possibility that these receptors could be co-distributed when they are co-expressed in HEK293T cells. The co-expression of D_1 and $CRF_{2\alpha}$ receptors drastically changed their subcellular distribution pattern (Figure 2). D_1 $receptors^{YFP}$ acquired a higher intracellular phenotype in cells co-expressing $CRF_{2\alpha}$ $receptor^{CFP}$ showing a pattern similar to $CRF_{2\alpha}$ $receptor^{CFP}$ yielding a high degree of superposition of both labels (Figure 2A). Consistently, a Pearson's coefficient of 0.86 ± 0.01 was obtained indicating that both receptors exhibited a high degree of co-localization. Interestingly, in some cells that expressed only D_1 $receptor^{YFP}$, in the same preparation, the surface phenotype of D_1 $receptor^{YFP}$ was preserved (Figure 2A, asterisk). These data indicate that $CRF_{2\alpha}$ $receptor^{CFP}$ drags D_1 $receptor^{YFP}$ to the intracellular compartment, suggesting the formation of a heteromeric complex between D_1 and $CRF_{2\alpha}$ receptors. Figure 2B shows the quantification of the percentage of cells showing surface or intracellular D_1 $receptor^{YFP}$ phenotype when expressed alone or with $CRF_{2\alpha}$ $receptor^{CFP}$. A significant decrease in the percentage of cells expressing D_1 $receptor^{YFP}$ in the surface and a concomitant increase in the intracellular compartment was observed when D_1 $receptor^{YFP}$ was co-expressed with $CRF_{2\alpha}$ $receptor^{CFP}$. In order to evaluate the specificity of the $CRF_{2\alpha}$ $receptor^{CFP}$ induced-retention of D_1 $receptor^{YFP}$ in the

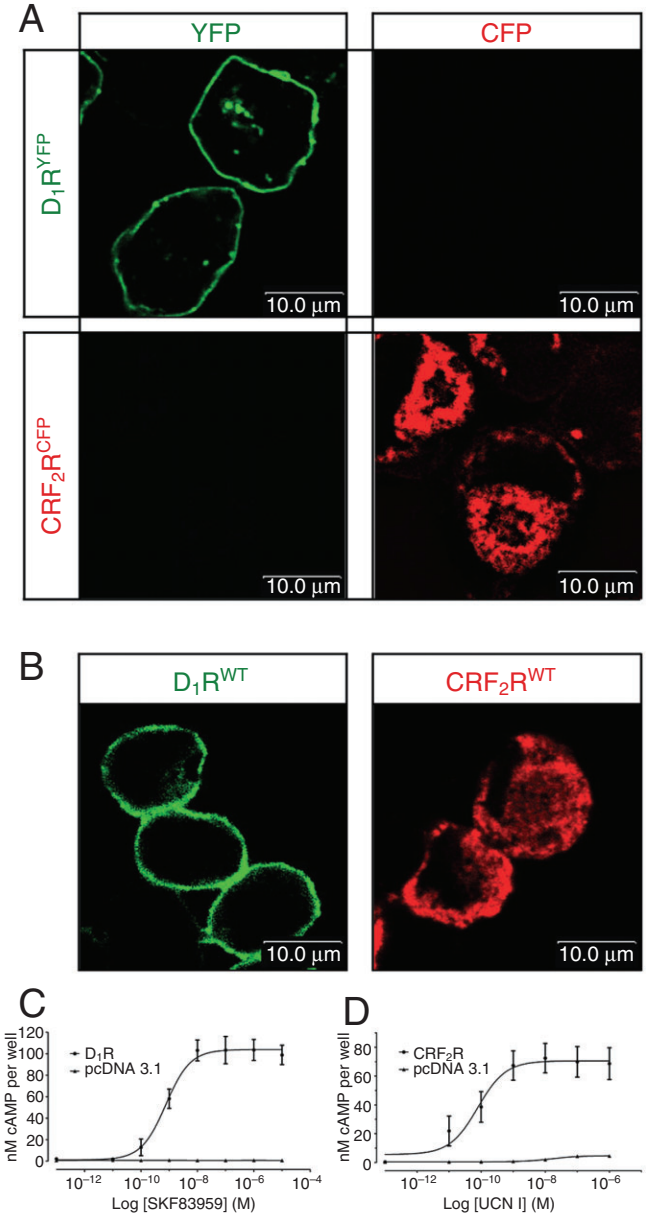

Figure 1

Subcellular distribution pattern of D_1 and $CRF_{2\alpha}$ receptors expressed in HEK293T cells. (A) Fluorescence of chimeric proteins. D_1 receptor^{YFP} and $CRF_{2\alpha}$ receptor^{CFP} expressed in HEK293T-cells, fluorescence images of YFP and CFP were obtained by confocal microscopy. The upper panel shows the surface fluorescence of D_1 receptor^{YFP}, and the bottom panel shows the intracellular fluorescence of $CRF_{2\alpha}$ receptor^{CFP}. (B) Immunofluorescence of wild-type receptors. D_1 receptor (left) and $CRF_{2\alpha}$ receptor (right) were detected by immnunofluorescence. Six fields of cells per independent experiment (n = 3) were examined. Individual cells were classified as having either fluorescence almost exclusively in a bright ring surrounding the cell (surface), or dense intracellular fluorescence (intracellular). Data are expressed as mean ± SEM and represent results from about 200 cells. *$P \leq 0.05$, Mann–Whitney test. Scale bar: 10 µm. (C–D) Concentration–response curves showing cAMP levels. Cells expressing D_1 receptors were stimulated with increasing concentration of SKF83959 (C); data are expressed as mean ± SEM (n = 3). Cells expressing $CRF_{2\alpha}$ receptors were stimulated with increasing concentration of urocortin (UCN)I (D), data are expressed as mean ± SEM (n = 6).

intracellular compartment, HEK293T cells, were co-transfected either with CRF_1 receptor^{YFP} or CRF_1 receptor^{YFP} plus $CRF_{2\alpha}$ receptor^{CFP}. CRF_1 receptor^{YFP} expressed alone presented a surface phenotype (data not shown) and its distribution was not changed when both CRF_1 receptor^{YFP} and $CRF_{2\alpha}$ receptor^{CFP} were co-expressed (Figure 2C), further proving that the effect of $CRF_{2\alpha}$ receptor over D_1 receptor localization was specific.

Heteromerization of D_1R and $CRH_{2\alpha}R$

To confirm that D_1 and $CRF_{2\alpha}$ receptors physically interact, co-immuneprecipitation, BRET and FRET assays were performed in HEK293T cells. D_1 receptors and $CRF_{2\alpha}$ receptors were shown to physically interact.

Co-immunoprecipitation experiments were performed, as a classical biochemical approach. Interestingly, $CRF_{2\alpha}$ receptor^{Flag} (band of ~70 kDa) was able to co-immunoprecipate together with D_1 receptor$^{myc/His}$ using a rabbit anti-myc polyclonal antibody, only from extracts of cells transiently transfected with D_1 receptor$^{myc/His}$ plus $CRF_{2\alpha}$ receptor^{Flag} (Figure 3A, IP: lane 3). In addition, a higher molecular weight band (~130 kDa) was observed. Importantly, these bands did not appear in immunoprecipitates of proteins extracted from cells transfected with D_1 receptor$^{myc/His}$ (lane 1), $CRF_{2\alpha}$ receptor^{Flag} (lane 2) or the empty pcDNA vector (lane 4). Finally, the presence of D_1 receptors in the crude extracts was confirmed by Western blot using a rabbit polyclonal antibody against c-myc (Figure 3A, right). Overall, these results showed that D_1 and $CRF_{2\alpha}$ receptors form a protein complex.

Next, the ability of D_1 and $CRF_{2\alpha}$ receptors to heteromerize was evaluated using biophysical approaches. Accordingly, the degree of $D_1/CRF_{2\alpha}$ receptor interaction was analysed by means of BRET experiments (Figure 3B). Thus, a BRET saturation curve was constructed in HEK293T cells co-transfected with a constant amount of $CRF_{2\alpha}$ receptor^{Rluc} and increasing concentrations of D_1 receptor^{YFP}, D_2 receptor^{YFP} or $GABA_{B2}$ receptor^{YFP}. Interestingly, a positive BRET signal was obtained between $CRF_{2\alpha}$ receptor^{Rluc} and D_1 receptor^{YFP}. As shown in Figure 3B, the BRET ratio between $CRF_{2\alpha}$ receptor^{Rluc} and D_1 receptor^{YFP} increased as a hyperbolic function of the concentration of the D_1 receptor^{YFP}. Importantly, the pairing of $CRF_{2\alpha}$ receptor^{Rluc} with D_2 receptor^{YFP} led to a non-significant BRET signal, which was within the same range as that observed for the $CRF_{2\alpha}$ receptor^{Rluc}/$GABA_{B2}$ receptor^{YFP} pair (i.e. non-specific), thus supporting the specificity of the $CRF_{2\alpha}$ receptor^{Rluc}/D_1 receptor^{YFP} interaction.

Additionally, the formation of $D_1/CRF_{2\alpha}$ receptor heteromers was also assessed by means of FRET experiments. To this end, cells were transiently transfected with D_1 receptor^{YFP} and $CRF_{2\alpha}$ receptor^{CFP}, and their ability to heteromerize was determined by calculating the FRET efficiency using the donor recovery after acceptor bleaching approach (Fig. 3C). The formation of $D_1/CRF_{2\alpha}$ receptor heteromers is indicated by the resonance energy transfer between the fluorescent proteins, which was measured by the recovery of the CFP emission after photobleaching of YFP (Figure 3C). The application of the photobleaching protocol to cells expressing only $CRF_{2\alpha}$ receptor^{CFP} did not modify the emission intensity of CFP (Figure 3D). As additional controls, to ensure that the FRET signal was due to a specific interaction and not to a random proximity of the fluorophores, FRET efficiency was

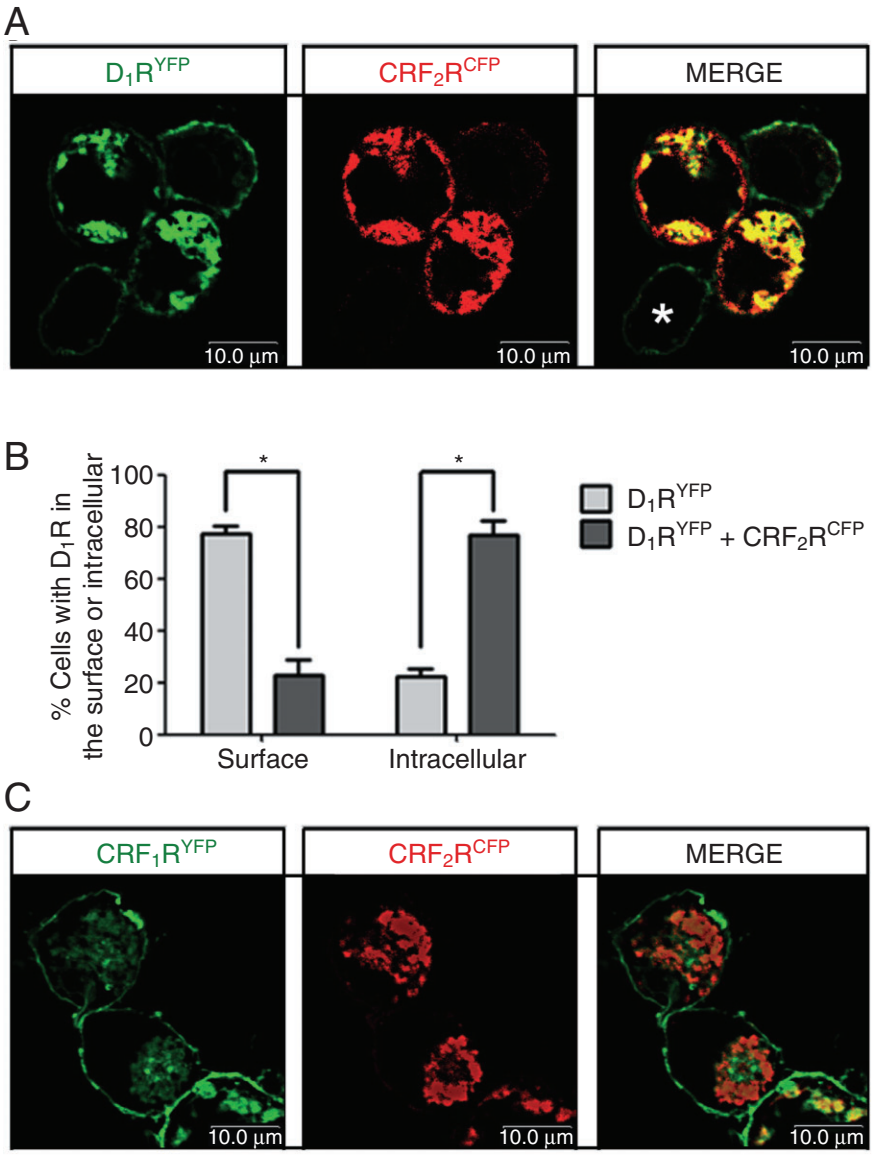

Figure 2

D_1 receptor^{YFP} and $CRF_{2\alpha}$ receptor^{CFP} mutually modify their subcellular distribution when they are co-expressed. (A) Co-expression of chimeric protein D_1 receptor^{YFP} and $CRF_{2\alpha}$ receptor^{CFP} in HEK293T cells. Six fields of cells per independent experiment ($n = 3$) were examined. D_1 receptor^{YFP} acquires an intracellular phenotype in cells co-expressing $CRF_{2\alpha}$ receptor^{CFP}, with high degree of co-distribution in the merge. The cells that only expressed D_1 receptor^{YFP} maintained their surface phenotype (asterisk). (B) Quantification of surface and intracellular phenotypes when D_1 receptor^{YFP} is expressed alone or with $CRF_{2\alpha}$ receptor^{CFP}. The percentage of cells with receptors at the cell surface is greater when D_1 receptor^{YFP} was expressed alone, lower when $CRF_{2\alpha}$ receptor^{CFP} was expressed alone, and an intermediate level was obtained when the receptors where co-expressed. Data are expressed as mean ± SEM and represent results from about 200 cells of three independent experiments ($n = 3$) *$P \leq 0.05$, Mann–Whitney test. (C) Co-expression of CRF_1 receptor^{YFP} and $CRF_{2\alpha}$ receptor^{CFP}. The subcellular localization of both receptors is maintained.

determined in cells co-expressing $CRF_{2\alpha}$ receptor^{CFP} plus YFP, D_1 receptor^{YFP} plus CFP or $CRF_{2\alpha}$ receptor^{CFP} plus D_2 receptor^{YFP}, at comparable fluorescence levels. Under these experimental conditions the FRET efficiency of the $CRF_{2\alpha}$ receptor^{CFP}/D_1 receptor^{YFP} pair was significantly higher (9.65 ± 1.07; $P < 0.001$) than that observed in the corresponding negative controls (i.e. $CRF_{2\alpha}$ receptor^{CFP}/YFP and CFP/D_1 receptor^{YFP} pairs) (Figure 3D). Interestingly, the FRET efficiency of the $CRF_{2\alpha}$ receptor^{CFP} and D_2 receptor^{YFP} pair was not significantly different from that observed for the other negative controls used (Figure 3D). Overall, these results strongly suggest that D_1 and $CRF_{2\alpha}$ receptors physically interact in living cells.

D_1 receptor and $CRF_{2\alpha}$ receptor form a stable heteromer

In order to further test the capacity of D_1 and $CRF_{2\alpha}$ receptors to physically interact and the stability of the heteromer, we used the heteromer mobilization strategy described by O'Dowd *et al.* (2005) associated with immunofluorescence for

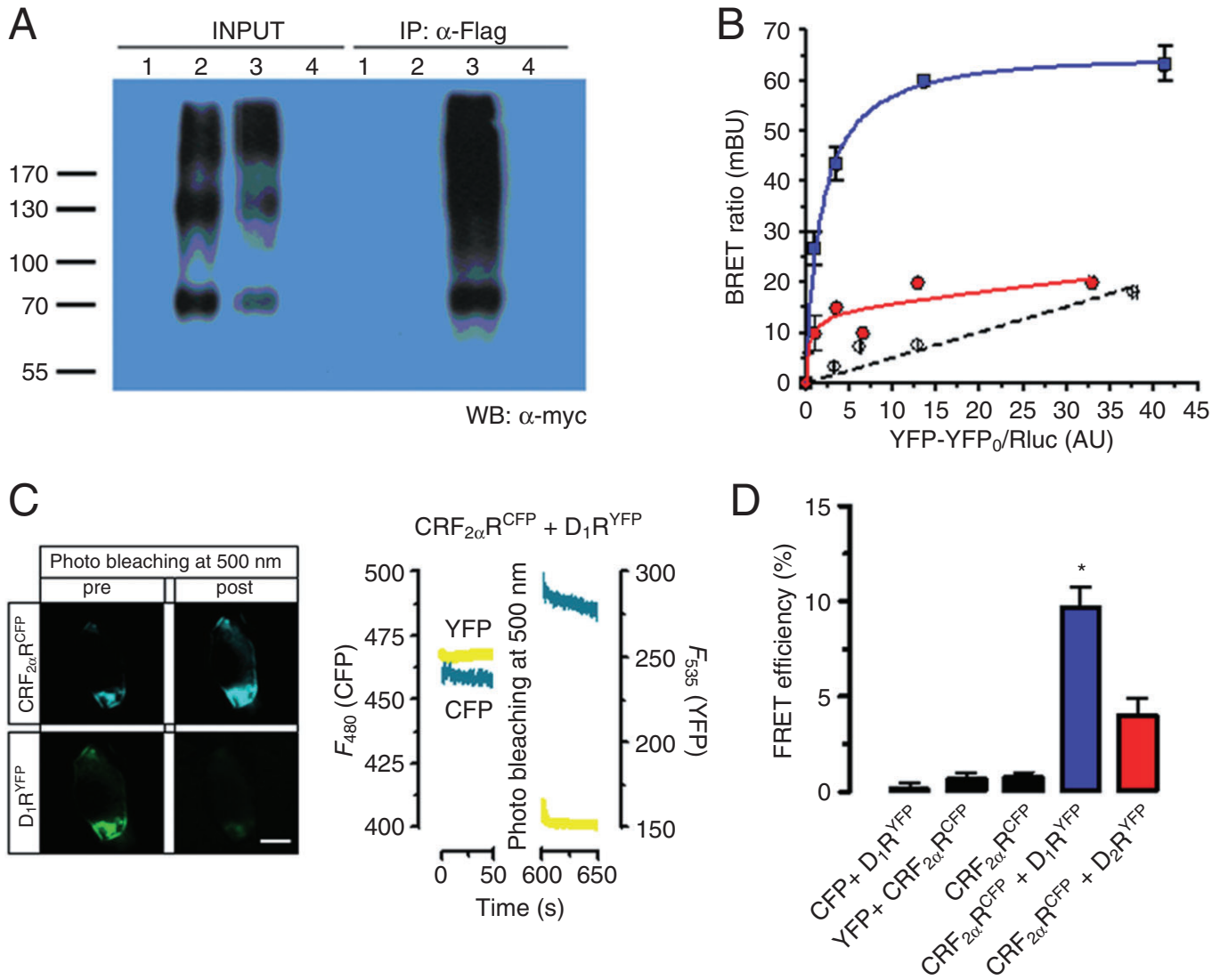

Figure 3

Heteromerization of D_1 receptors and $CRF_{2\alpha}$ receptors. (A) Co-immunoprecipitation of D_1 receptor$^{myc/His}$ and $CRF_{2\alpha}$ receptor^{Flag} from HEK293T cells. Solubilized extracts from cells expressing D_1 receptor$^{myc/His}$ (lane 1), $CRF_{2\alpha}$ receptor^{Flag} (lane 2), D_1 receptor$^{myc/His}$ plus $CRF_{2\alpha}$ receptor^{Flag} (lane 3) or empty pcDNA 3.1 vector (lane 4) were immunoprecipitated with a rabbit anti-myc polyclonal antibody. Extracts (crude) and immunoprecipitates (IP) were analysed using a mouse anti-Flag and a rabbit anti c-myc antibodies. $CRF_{2\alpha}$ receptor^{Flag} immunoprecipitated with D_1 receptor$^{myc/His}$ (IP, lane 3). The presence of D_1 receptor$^{myc/His}$ was corroborated (lanes 1 and 3). (B) BRET saturation curve. BRET was measured in HEK293T cells co-expressing $CRF_{2\alpha}$ receptor^{Rluc} plus D_1 receptor^{YFP} (blue squares), $CRF_{2\alpha}$ receptor^{Rluc} plus D_2 receptor^{YFP} (red circles) or $CRF_{2\alpha}$ receptor^{Rluc} plus $GABA_{B2}$ receptor^{YFP} (black circles). Co-transfections were performed with increasing amounts of the YFP-tagged vectors while the $CRF_{2\alpha}$ receptor^{Rluc} was maintained constant. Plotted on the X-axis is the fluorescence value obtained from the YFP, normalized to the luminescence value of $CRF_{2\alpha}$ receptor^{Rluc} 10 min after *h*-coelenterazine incubation. (C) Determination of the D_1 and $CRF_{2\alpha}$ receptor oligomerization by FRET experiments in living cells. D_1 receptor^{YFP} and $CRF_{2\alpha}$ receptor^{CFP} were expressed in HEK293T cells, and fluorescence images of CFP and YFP were recorded before (pre) and after (post) the YFP was photobleached by 5 min of exposure to light at 500 nm to corroborate the extent of acceptor photodestruction (left panel). Emission intensities of $CRF_{2\alpha}$ receptor^{CFP} (480 nm, blue) and D_1 receptor^{YFP} (535 nm, yellow) from single cells expressing both $CRF_{2\alpha}$ receptor^{CFP} and D_1 receptor^{YFP} were recorded before and after YFP photobleaching (right panel) to determine the FRET efficiency. Scale bar: 10 μm. (D) Quantification of the FRET efficiency of different FRET pairs: CFP plus D_1 receptor^{YFP} ($n = 5$), YFP plus $CRH_{2\alpha}R^{CFP}$ ($n = 10$), $CRH_{2\alpha}R^{CFP}$ ($n = 5$), D_1R^{YFP} plus $CRF_{2\alpha}$ receptor^{CFP} ($n = 15$) and D_2 receptor^{YFP} plus $CRF_{2\alpha}$ receptor^{CFP} ($n = 10$). The data indicate the mean ± SEM. An asterisk denotes the data that are significantly different from the control FRET pairs (i.e., CFP or YFP co-transfections). *$P < 0.001$, ANOVA with a Bonferroni multiple comparison *post hoc* test.

WGA^{647}, a cell surface marker. Briefly, this strategy involves the incorporation of a NLS to a given GPCR such that the GPCR acquires the unique property of being retained in the intracellular compartment in the absence of antagonist, and in the cell surface in the presence of inverse agonist/antagonist. Thus, the heteromeric interaction and its stability are evaluated analysing the co-trafficking of both receptors to the different subcellular compartments. As expected, the incorporation of the NLS sequence reported by O'Dowd *et al.* (2005) to D_1 receptor^{YFP} (D_1 receptor-NLS^{YFP}) conferred a mainly intracellular phenotype for D_1 receptor-NLS^{YFP} (≈90% of the cells, data not shown).

The use of immunofluorescence with WGA^{647} as marker of the cell surface confirmed that D_1 receptor^{YFP} fluorescence is mainly present at the cell surface meanwhile $CRF_{2\alpha}$ receptor^{CFP} is present mainly intracellularly (Figure 4A). Figure 4B shows the results obtained with the strategy of O'Dowd *et al.* (2005) co-expressing D_1 receptor^{YFP} plus $CRF_{2\alpha}$ receptor^{CFP} (Fig. 4Ba–c), D_1 receptor-NLS^{YFP} plus $CRF_{2\alpha}$ receptor^{CFP} (Figure 4Bd–f) and of D_1 receptor-NLS^{YFP} plus $CRF_{2\alpha}$ receptor^{CFP} in the presence of 1 μM SCH23390 (Figure 4Bg–i). Colocalization analysis showed that the incorporation of NLS to D_1 receptor^{YFP} decreased Pearson's correlation coefficient between CFP and WGA^{647} from 0.37 ± 0.02 to 0.02 ± 0.01, and the presence of 1 μM SCH23390 restored the cell surface expression of $CRF_{2\alpha}$ receptor^{CFP} up to a Pearson's correlation coefficient of 0.27 ± 0.02 (Figure 4C).

The percentage of cells with $CRF_{2\alpha}$ receptor^{CFP} at the cell surface was estimated comparing the localization of CFP fluorescence with WGA^{647}. When both receptors were co-expressed 41.8 ± 4.8% of cells presented $CRF_{2\alpha}$ receptor^{CFP} at the cell surface (Figure 4D). The incorporation of NLS to D_1 receptor^{YFP} (D_1 receptor-NLS^{YFP}) significantly decreased the percentage of cells with $CRF_{2\alpha}$ receptor^{CFP} at the cell surface indicating that D_1 receptor-NLS^{YFP} was physically interacting with $CRF_{2\alpha}$ receptor^{CFP} and was therefore able to drag $CRF_{2\alpha}$ receptor^{CFP} forcing the intracellular localization induced by NLS. The formation of a stable heteromer was further demonstrated in the presence of 1 μM SCH23390, a specific D_1 receptor antagonist/inverse agonist that is able to retain D_1 receptor-NLS^{YFP} at the cell surface. Indeed, in the presence of 1 μM SCH23390 a significant recovery in the percentage of cells expressing $CRF_{2\alpha}$ receptor^{CFP} at the cell surface was observed (Figure 4D). These data show that D_1 receptor^{YFP} and $CRF_{2\alpha}$ receptor^{CFP} form a stable heteromer.

As the intracellular fluorescence given by the D_1 /$CRF_{2\alpha}$ receptor heteromer looks like the cell reticular compartment, we analysed the colocalization of the receptors with calnexin,

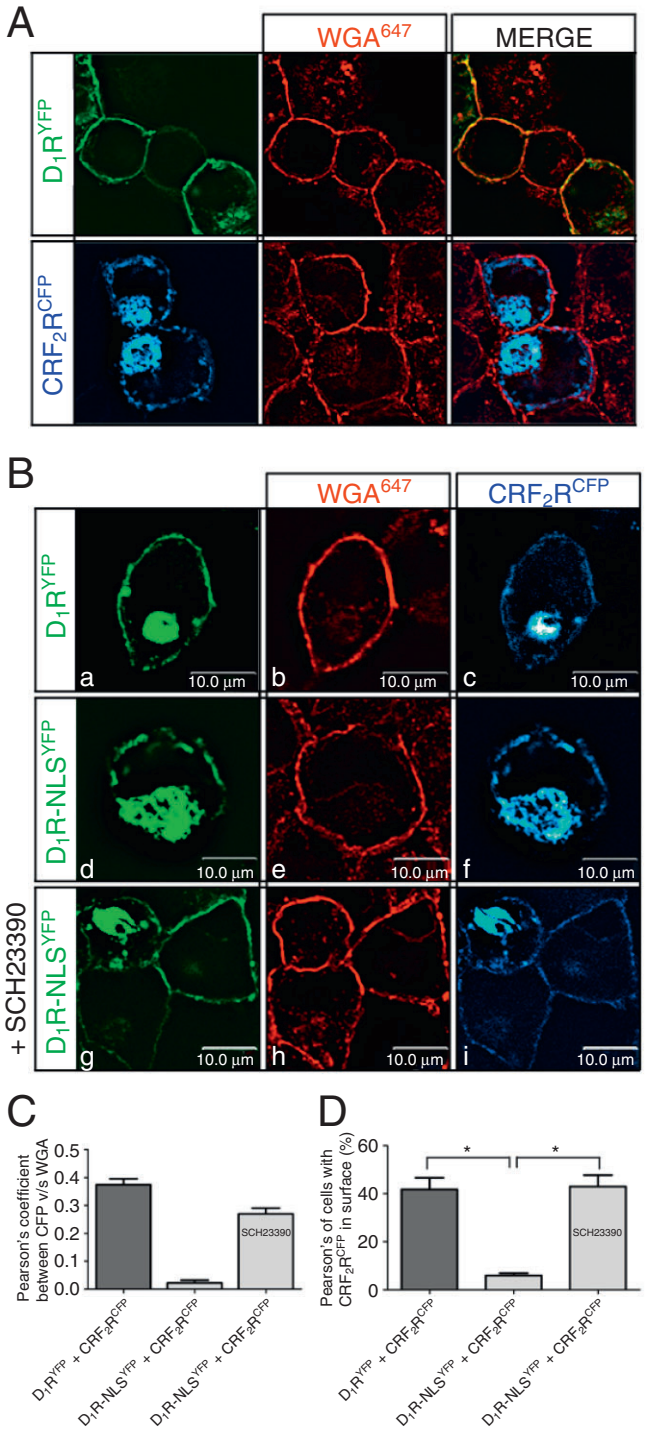

Figure 4

D_1 and $CRF_{2\alpha}$ receptors form a stable heteromeric complex in HEK293T cells. (A) Co-localization of $CRF_{2\alpha}$ receptor^{CFP} with the plasma membrane marker WGA^{647}, when it was co-expressed with: D_1 receptor^{YFP} (a–c), D_1 receptor-NLS^{YFP} (d–f) or D_1 receptor-NLS^{YFP} treated with SCH23390 (1 μM) (g–i). The number of $CRF_{2\alpha}$ receptors in the plasma membrane was augmented when it was co-expressed with D_1 receptor^{YFP} (a–c). When co-transfected with D_1 receptor-NLS^{YFP}, the $CRF_{2\alpha}$ receptor^{CFP} co-trafficked with the D_1 receptor-NLS^{YFP} to the intracellular compartment, being excluded from the plasma membrane (d–f). The treatment with SCH23390 (1 μM) to the cells co-transfected with D_1 receptor-NLS^{YFP} and $CRF_{2\alpha}$ receptor^{CFP} allowed both receptors to be observed at the cell surface (g–i). (B) Pearson's correlation coefficient between CFP and WGA^{647}. In each condition, the Pearson's coefficient was calculated from the different transfection conditions. Data are expressed as mean ± SEM and represent results from 18 to 30 cells of two independent experiments. (C) Quantification of the percentage of cells showing a surface phenotype for $CRF_{2\alpha}$ receptors. The percentage of cells was calculated in the different transfection conditions. Data are expressed as mean ± SEM and represent results from about 200 cells from three independent experiments (n = 3) *P ≤ 0.05, Mann–Whitney test.

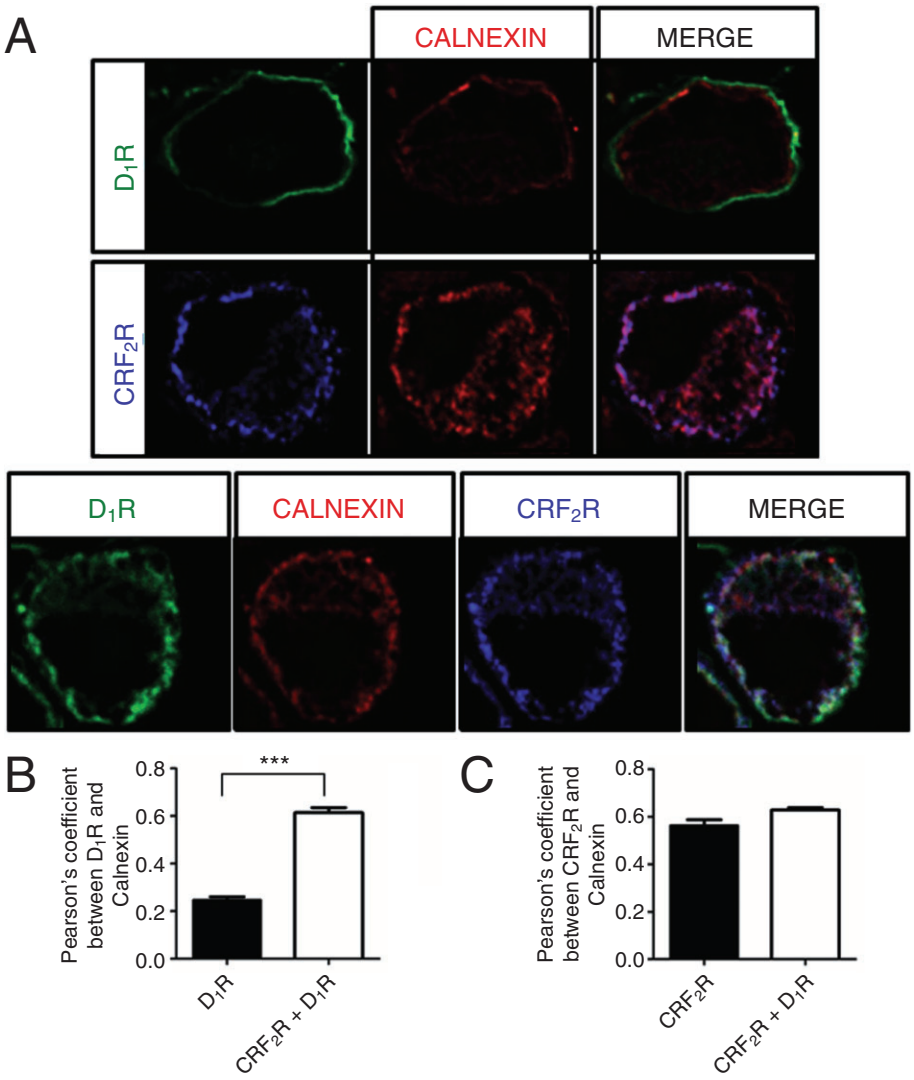

Figure 5

Colocalization of D_1 and $CRF_{2\alpha}$ receptors with calnexin, a marker of the cellular reticular compartment. (A) Immunofluoresence of D_1 receptor$^{myc/His}$ and $CRF_{2\alpha}$ receptors expressed alone or co-expressed in HEK293T cells and of calnexin. (B) Pearson's correlation coefficient between D_1 receptor$^{myc/His}$ and calnexin in the presence or absence of $CRF_{2\alpha}$ receptors ($P < 0.001$; Mann–Whitney test). (C) Pearson's correlation coefficient between $CRF_{2\alpha}$ receptors and calnexin in the presence or absence of D_1 receptor$^{myc/His}$.

a marker of the cellular reticular compartment. As can be seen in Figure 5A, cells transfected with D_1 receptor$^{myc/His}$ showed a poor colocalization with calnexin that significantly increased when D_1 receptor$^{myc/His}$ and $CRF_{2\alpha}$ receptor were co-expressed (Figure 5B). In contrast, immunofluorescence against $CRF_{2\alpha}$ receptor showed high colocalization with calnexin (Figure 5A) that did not significantly change when both receptors were co-expressed (Figure 5C).

D_1/$CRF_{2\alpha}$ receptor heteromer and cAMP signalling

In order to test whether the heteromerization between D_1 and $CRF_{2\alpha}$ receptors switch their cAMP signalling mode, we measured cAMP induced by increasing concentrations of SKF83959 (D_1 receptor agonist; Figure 6A) and urocortin I (CRF_2 receptor agonist; Figure 6B) in HEK293T cells transfected with D_1 receptors, $CRF_{2\alpha}$ receptors and D_1 plus $CRF_{2\alpha}$ receptors. As expected, the presence of SKF83959 induced a concentration-dependent increase in cAMP in D_1 receptor, but not $CRF_{2\alpha}$ receptor, expressing cells (Figure 6A). The D_1 receptor specificity of the response to SKF83959 was confirmed because HEK293T cells transfected with the empty vector did not show a response. Interestingly, SKF83959 induced the same level of response when both receptors were co-expressed. The presence of 10 μM SCH23390 displaced the SKF83959 concentration–response curve to the right obtained with both, D_1 receptor and D_1 plus $CRF_{2\alpha}$ receptor expressing cells further confirming the specificity of the response (Figure 6A).

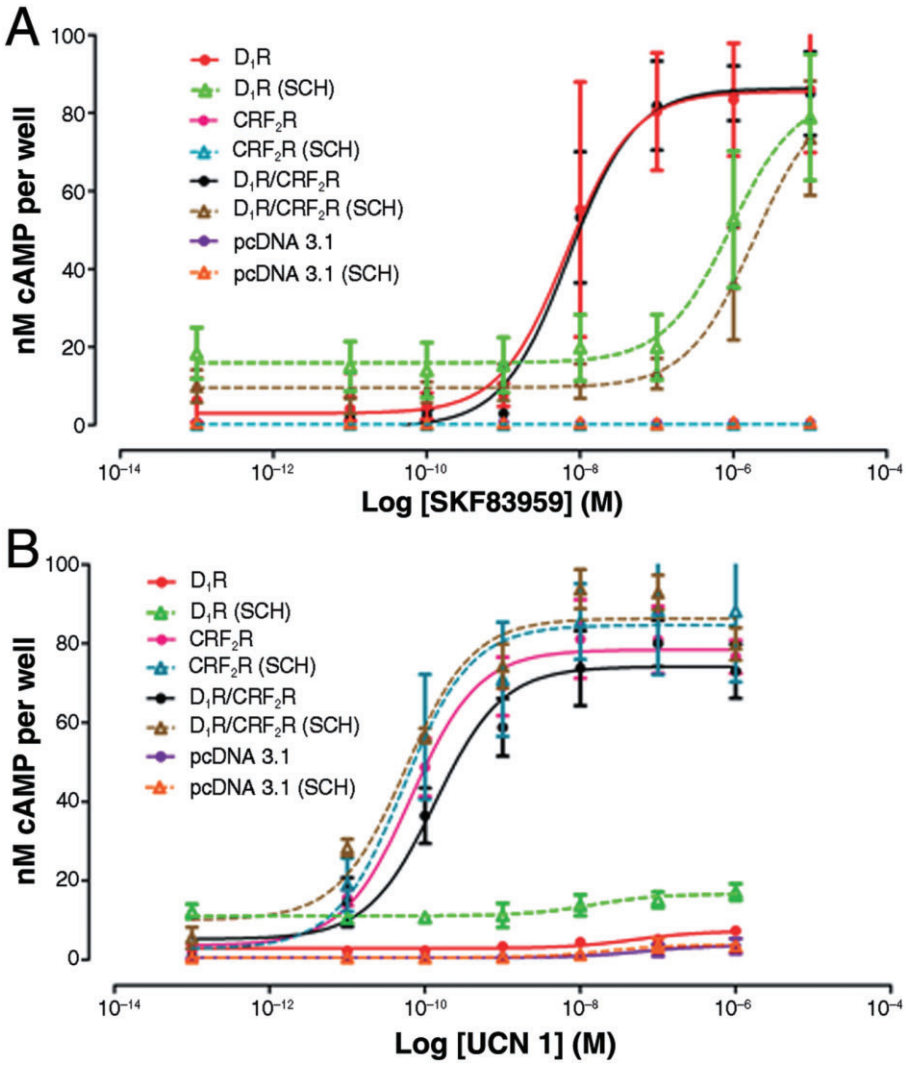

Figure 6

Concentration–response curves for cAMP accumulation. HEK293T cells expressing D_1 receptors and $CRF_{2\alpha}$ receptor alone and cells co-expressing D_1 plus $CRF_{2\alpha}$ receptors were incubated in the presence of different concentrations of SKF83959 (A) or urocortin (UCN) I (B) with or without 10 μM SCH23390 (SCH). The results are the mean ± SEM of three independent experiments.

The presence of urocortin I induced a concentration-dependent increase in cAMP in $CRF_{2\alpha}$ receptor, but not D_1 receptor expressing cells (Figure 6B). The $CRF_{2\alpha}$ receptor specificity of the response to urocortin I was confirmed because HEK293T cells transfected with the empty vector did not show a response. Similar to what was observed with SKF83959, the presence of urocortin I induced the same level of response when both receptors were co-expressed (Figure 6B). The presence of 10 μM SCH23390 displaced the SKF83959 concentration–response curve to the right obtained with both D_1 receptor and D_1 plus $CRF_{2\alpha}$ receptor-expressing cells further confirming the specificity of the response (Figure 6A). To test a possible crosstalk between both receptors, we determined cAMP accumulation induced by urocortin I in the presence of SCH23390. As can be seen in Figure 6B, the presence of 10 μM SCH23390 did not modify the urocortin I concentration–response curve. These data indicate that the heteromerization between both receptors does not modify cAMP signalling from each individual receptor.

D_1/$CRF_{2\alpha}$ receptor heteromer activation by dopamine agonists triggers calcium mobilization

HEK293T cells transfected with only D_1 receptors or D_1 plus $CRF_{2\alpha}$ receptors were loaded with FURA-2 AM and intracellular calcium mobilization was measured in a calcium-free medium. The addition of 10 μM SKF83959, a D_1 receptor agonist, to cells expressing only D_1 receptors triggered calcium mobilization in just one of the tested cells (n = 67), representing 1.5% of them. However, the addition of 10 μM SKF83959 to cells co-transfected with D_1 plus $CRF_{2\alpha}$ receptors, triggered calcium mobilization in 36.7% of the tested cells (n = 71) (Figure 7A–B). Mobilization of intracellular calcium

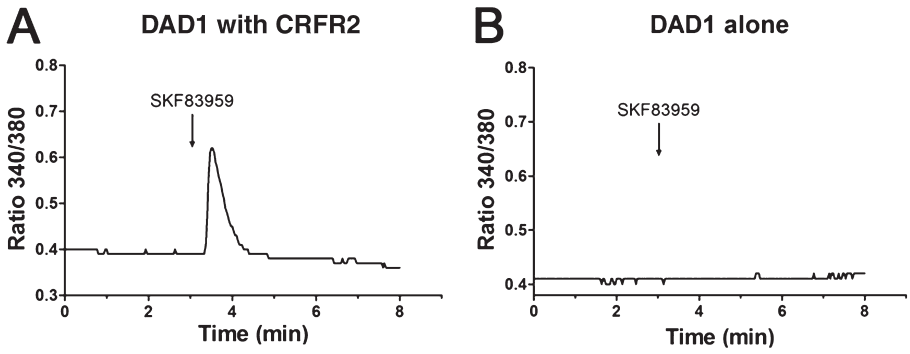

Figure 7

Calcium mobilization induced by the activation of D_1 receptors. HEK293T cells expressing D_1 receptors alone or D_1 plus $CRF_{2\alpha}$ receptors were loaded with FURA-2 AM. Intracellular calcium mobilization was measured in living cells at 340 and 380 nm in a confocal microscope and time lapse of the 340/380 ratio was plotted. The selective D_1 receptor agonist, SKF83959, generated calcium mobilization when the receptors were co-expressed (n = 71), but no effect was observed when D_1 receptors were expressed alone (n = 67). The data were obtained from four independent experiments.

in response to the ionophore ionomycin was measured in each tested cell to determine cell responsiveness (data not shown).

Discussion and conclusions

In the present study, we show that D_1 receptors and $CRF_{2\alpha}$ receptors are capable of forming a stable heteromer in living cells, modifying their subcellular localization and signalling. Each receptor has a distinct subcellular localization, the D_1 receptor being mainly at the cell surface and $CRF_{2\alpha}$ receptor mostly intracellular. Interestingly, when both receptors were co-expressed, a balanced subcellular localization for both receptors was observed, thus suggesting that D_1 and $CRF_{2\alpha}$ receptors heteromerize. We demonstrated the existence of D_1/$CRF_{2\alpha}$ receptor heteromers by co-immunoprecipitation, BRET and FRET assays. Furthermore, we show that D_1 and $CRF_{2\alpha}$ receptors form a stable heteromer using the heteromer mobilization strategy described by O'Dowd *et al.* (2005). In addition, we showed that the heteromerization of D_1 receptors with $CRF_{2\alpha}$ receptors switches the signalling of D_1 receptors from a receptor that does not mobilize intracellular calcium to a receptor that mobilizes intracellular calcium. Thus, our results indicate that the heteromerization of D_1 receptors and $CRF_{2\alpha}$ receptors has at least two fundamental functional implications: (1) change in the subcellular localization of both receptors and (2) change in the signalling cascade associated with D_1 receptor stimulation.

Our results show that transfected $CRF_{2\alpha}$ receptors were mainly located intracellularly (≈85%); similar to what is has been observed in neurons of the rat dorsal raphe nucleus (Waselus *et al.*, 2009). There are other GPCRs that are constitutively intracellular such as $GABA_{B1}$ receptors (Margeta-Mitrovic *et al.*, 2000), CB_1 receptors (Andersson *et al.*, 2003), α_{1D}-adrenoceptors (Hague *et al.*, 2004a) and 5-$HT_{2A/C}$ (Magalhaes *et al.*, 2010) receptors. Interestingly, Markovic *et al.* (2008) have shown that the β isoform of the CRF_2 receptor is constitutively present in the cell surface, in contrast to what we observed with the $CRF_{2\alpha}$ receptor. The α and β isoforms of the CRF_2 receptor differ in their N-terminal sequence (Grigoriadis *et al.*, 1996). It has been shown that the rat $CRF_{2\alpha}$ receptor has a non-cleavable pseudo signal peptide of 19-aminoacids in the N-terminal (Rutz *et al.*, 2006), and that the lack of its cleavage affects the expression and traffic of $CRF_{2\alpha}$ receptors to the plasma membrane (Schulz *et al.*, 2010; Teichmann *et al.*, 2012). Interestingly, Teichmann *et al.* (2012) have shown that the rat $CRF_{2\alpha}$ receptor does not dimerize and have determined that this is due to its non-cleavable N-terminal pseudo signal peptide. Our data suggest that the presence of the pseudo signal peptide is not an impediment for the heteromerization of $CRF_{2\alpha}$ receptors with a class A GPCR such as the D_1 receptor. The 19-amino acid N-terminal segment of the $CRF_{2\alpha}$ receptor is highly conserved among several species. Therefore, it is not surprising that the human $CRF_{2\alpha}$ receptor studied herein is also found mainly intracellularly. Other receptors like α_{1D}-adrenoceptors (Hague *et al.*, 2004a) and CB_1 receptors (Andersson *et al.*, 2003) also have an intracellular localization that depends on their N-terminal. As stated before, the CRF_2 receptor was found predominantly in the cytoplasm in neurons of the rat dorsal raphe nucleus (Waselus *et al.*, 2009). Even though the CRF_2 receptor antibody used by Waselus *et al.* (2009) might not discriminate between both CRF_2 receptor isoforms (Lukkes *et al.*, 2011), their study relates to the $CRF_{2\alpha}$ receptor, as it has been shown the $CRF_{2\alpha}$ isoform is present in neurons and the $CRF_{2\beta}$ receptor in non-neuronal cells in the CNS (Chalmers *et al.*, 1995; Lovenberg *et al.*, 1995; Dautzenberg and Hauger, 2002). In contrast to $CRF_{2\alpha}$ receptor, and as has been previously shown (Vickery and von Zastrow, 1999; O'Dowd *et al.*, 2005; Sun *et al.*, 2009), the transfected D_1 receptor presented a surface phenotype.

Our results show that the heteromerization between D_1 and $CRF_{2\alpha}$ receptors alters the subcellular localization of both receptors. The need for a GPCR partner to traffic to another subcellular compartment has been previously demonstrated for other GPCRs (Kaupmann *et al.*, 1998; Margeta-Mitrovic *et al.*, 2000). We observed that the $CRF_{2\alpha}$ receptor decreases

the surface phenotype of the D_1 receptor to an intermediate surface/intracellular phenotype. There is evidence that when the D_1 receptor heteromerizes with the D_2 receptor, the D_1 receptor also acquires an intermediate phenotype (So *et al.*, 2005). In this case, the heteromerization increases the presence of D_2 receptors and decreases the presence of D_1 receptors in the cell surface. We also showed that heteromerization between D_1 and $CRF_{2\alpha}$ receptors promotes the trafficking of $CRF_{2\alpha}$ receptors to the plasma membrane. Likewise, the D_1 receptor improves the trafficking of μ-opioid receptors (Juhasz *et al.*, 2008) and α_{1B}-adrenoceptor improves the trafficking of α_{1D}-adrenoceptors to the cell surface (Hague *et al.*, 2004a). Thus, the aforementioned findings, as well as the present study, suggest that the increased trafficking of $CRF_{2\alpha}$ receptors to the cell surface and of D_1 receptors to the intracellular compartment depends on the interaction between them. It is tempting to speculate that the changes in subcellular localization of CRF_2 receptors observed in the dorsal raphe after stress could be due to its heteromerization with another GPCR (Waselus *et al.*, 2009).

The heteromer mobilization strategy described by O'Dowd *et al.* (2005) allowed us to further prove that D_1 and $CRF_{2\alpha}$ receptors are capable of forming a stable heteromer. In the presence of the NLS sequence in the D_1 receptor, co-expressed D_1 receptor-NLS and the $CRF_{2\alpha}$ receptor function as a unit present at the cell surface and internalizes as such, in the presence or absence of the D_1 receptor antagonist respectively.

Finally, we demonstrated that the heteromerization of D_1 with $CRF_{2\alpha}$ receptors conferred the property of mobilizing intracellular calcium. Cells expressing D_1 receptors alone are not capable of mobilizing calcium. In contrast, when the D_1 receptor is co-expressed with the $CRF_{2\alpha}$ receptor, intracellular calcium mobilization is induced by the presence of a D_1 receptor agonist. Interestingly, our results show a strong parallel between the heteromerization of D_1 with D_2 receptors and of D_1 with $CRF_{2\alpha}$ receptors, not only at the subcellular distribution level mentioned earlier, but also at the functional level. Similar to what we observed for D_1 and $CRF_{2\alpha}$ receptors, it has been shown that the capacity of D_1 receptors to mobilize intracellular calcium depends on the formation of a stable D_1/D_2 receptor heteromer (Lee *et al.*, 2004; Hasbi *et al.*, 2009; 2010). It has been shown that the change in signalling pathway of the D_1 receptor in the D_1/D_2 receptor heteromer is due to a change in the GPCRs, from $G_{\alpha s}$ to $G_{\alpha q/11}$ (Lee *et al.*, 2004; Rashid *et al.*, 2007; Hasbi *et al.*, 2010; Verma *et al.*, 2010). However, there is also evidence that the change in D_1 receptor signalling may also be due to downstream signalling pathways that do not depend on the heteromerization (Chun *et al.*, 2013). There is also evidence of other GPCRs in which the heteromerization switches the GPCRs (George *et al.*, 2000; Mellado *et al.*, 2001; Charles *et al.*, 2003; Ferrada *et al.*, 2009). Thus, it is possible that the calcium mobilization associated with the activation of D_1 receptors when D_1 receptors are co-expressed with $CRF_{2\alpha}$ receptors is due to a change in the GPCRs. Further studies should address whether the change in intracellular calcium mobilization induced by the activation of D_1 receptors co-expressed with $CRF_{2\alpha}$ receptors is due to a change in its affinity for Gq (Hasbi *et al.*, 2009) or is due to a downstream crosstalk (Chun *et al.*, 2013), as has been shown for the D_1/D_2 receptor heteromer.

The functional implications of the existence of D_1/ $CRF_{2\alpha}$ receptor heteromers *in vivo* are presently unknown. However, there are several anatomical substrates such as the prefrontal cortex, amygdala, bed nucleus of the stria terminalis, lateral septum and VTA where these two receptors could be co-expressed in neurons and/or nerve terminals (Corominas *et al.*, 2010; Gysling, 2012). It is tempting to speculate that the $D_1/CRF_{2\alpha}$ receptor heteromer could be responsible for the potentiation of glutamatergic transmission from the basolateral amygdala to medial prefrontal cortex (Orozco-Cabal *et al.*, 2008) and for the switch from inhibition to facilitation of $CRF_{2\alpha}$ receptors observed in the lateral septum of rats repeatedly treated with cocaine (Liu *et al.*, 2005).

In summary, we showed that D_1 and $CRF_{2\alpha}R$ receptors are capable of forming a stable heteromer with functional implications, such as changes in the subcellular localization of both receptors and in the signalling of D_1 receptors. We would like to suggest that the existence of a $D_1/CRF_{2\alpha}$ receptor heteromer might explain, at least in part, the complex physiological interactions established between dopamine and CRH in normal and pathological conditions such as addiction, representing a new potential pharmacological target.

Acknowledgements

Supported by FONDECYT (grants N° 1070340, 1110392, 7070246 and 7080124); and Millenium Science Initiative MSI (grants N° P06/008-F and P10/063-F). K. A. A., E. H. B. and P. G. S. were recipients of doctoral fellowships from CONICYT, Chile. K. A. A. was a recipient of a travel award from CONICYT. This work was also supported by grants SAF2011-24779 and Consolider-Ingenio CSD2008-00005 from MINECO and ICREA Academia-2010 from the Catalan Institution for Research and Advanced Studies (ICREA) to F. C. We thank the collaboration of Ms Cledi C Cerda for the cAMP accumulation studies. We acknowledge FONDECYT grant N° 1130079, which made it possible to perform the cAMP accumulation studies.

List of author contributions

J. F., P. G., K. A. A. and P. G. S. designed and performed experiments and analysed data. E. H. B. designed experiments and advised on the quantitative analysis of protein expression studies. J. M. C. advised on the design and analysis of calcium signalling studies. J. F., P. G. and P. G. S. wrote the manuscript. F. C. directed and coordinated the FRET and BRET experiments. K. G. directed and coordinated the transfection and signalling studies. All authors contributed on the editing of the manuscript.

Conflicts of interest

The authors declare no conflict of interest.

References

Alexander SP, Benson HE, Faccenda E, Pawson AJ, Sharman JL, McGrath JC *et al.* (2013a). The concise guide to PHARMACOLOGY 2013/14: overview. Br J Pharmacol 170: 1449–1458.

Alexander SP, Benson HE, Faccenda E, Pawson AJ, Sharman JL, McGrath JC *et al.* (2013b). The concise guide to PHARMACOLOGY 2013/14: G-protein coupled receptors. Br J Pharmacol 170: 1459–1581.

Andersson H, D'Antona AM, Kendall DA, Von Heijne G, Chin CN (2003). Membrane assembly of the cannabinoid receptor 1: impact of a long N-terminal tail. Mol Pharmacol 64: 570–577.

Blanco EH, Zuñiga JP, Andres ME, Alvarez AR, Gysling K (2011). Corticotropin-releasing factor binding protein enters the regulated secretory pathway in neuroendocrine cells and cortical neurons. Neuropeptides 45: 273–279.

Bolte S, Cordelieres FP (2006). A guided tour into subcellular colocalization analysis in light microscopy. J Microsc 224: 213–232.

Burgueño J, Enrich C, Canela EI, Mallol J, Lluis C, Franco R *et al.* (2003). Metabotropic glutamate type 1alpha receptor localizes in low-density caveolin-rich plasma membrane fractions. J Neurochem 86: 785–791.

Cadet JL, Brannock C, Ladenheim B, McCoy MT, Krasnova IN, Lehrmann E *et al.* (2014). Enhanced upregulation of CRH mRNA expression in the nucleus accumbens of male rats after a second injection of methamphetamine given thirty days later. PLoS ONE 9: e84665.

Canals M, Marcellino D, Fanelli F, Ciruela F, de Benedetti P, Goldberg SR *et al.* (2003). Adenosine A2A-dopamine D2 receptor-receptor heteromerization: qualitative and quantitative assessment by fluorescence and bioluminescence energy transfer. J Biol Chem 278: 46741–46749.

Chalmers DT, Lovenberg TW, De Souza EB (1995). Localization of novel corticotropin-releasing factor receptor (CRF2) mRNA expression to specific subcortical nuclei in rat brain: comparison with CRF1 receptor mRNA expression. J Neurosci 15: 6340–6350.

Charles AC, Mostovskaya N, Asas K, Evans CJ, Dankovich ML, Hales TG (2003). Coexpression of delta-opioid receptors with micro receptors in GH3 cells changes the functional response to micro agonists from inhibitory to excitatory. Mol Pharmacol 63: 89–95.

Chun LS, Free RB, Doyle TB, Huang XP, Rankin ML, Sibley DR (2013). D1-D2 dopamine receptor synergy promotes calcium signaling via multiple mechanisms. Mol Pharmacol 84: 190–200.

Ciruela F, Burgueño J, Casadó V, Canals M, Marcellino D, Goldberg SR *et al.* (2004). Combining mass spectrometry and pull-down techniques for the study of receptor heteromerization. Direct epitope-epitope electrostatic interactions between adenosine A2A and dopamine D2 receptors. Anal Chem 76: 5354–5363.

Ciruela F, Fernández-Dueñas V, Llorente J, Borroto-Escuela D, Cuffí ML, Carbonell L *et al.* (2012). G protein-coupled receptor oligomerization and brain integration: focus on adenosinergic transmission. Brain Res 1476: 86–95.

Corominas M, Roncero C, Casas M (2010). Corticotropin releasing factor and neuroplasticity in cocaine addiction. Life Sci 86: 1–9.

Dautzenberg FM, Hauger RL (2002). The CRF peptide family and their receptors: yet more partners discovered. Trends Pharmacol Sci 23: 71–77.

Ferrada C, Moreno E, Casadó V, Bongers G, Cortés A, Mallol J *et al.* (2009). Marked changes in signal transduction upon heteromerization of dopamine D1 and histamine H3 receptors. Br J Pharmacol 157: 64–75.

George O, Le Moal M, Koob GF (2012). Allostasis and addiction: role of the dopamine and corticotropin-releasing factor systems. Physiol Behav 106: 58–64.

George SR, Fan T, Xie Z, Tse R, Tam V, Varghese G *et al.* (2000). Oligomerization of mu- and delta-opioid receptors. Generation of novel functional properties. J Biol Chem 275: 26128–26135.

Grigoriadis DE, Lovenberg TW, Chalmers DT, Liaw C, De Souze EB (1996). Characterization of corticotropin-releasing factor receptor subtypes. Ann N Y Acad Sci 780: 60–80.

Guan X, Wan R, Zhu C, Li S (2014). Corticotropin-releasing factor receptor type-2 is involved in the cocaine-primed reinstatement of cocaine conditioned place preference in rats. Behav Brain Res 258: 90–96.

Gutknecht E, Hauger RL, Van der Linden I, Vauquelin G, Dautzenberg FM (2008). Expression, binding, and signaling properties of CRF2(a) receptors endogenously expressed in human retinoblastoma Y79 cells: passage-dependent regulation of functional receptors. J Neurochem 104: 926–936.

Gysling K (2012). Relevance of both type-1 and type-2 corticotropin releasing factor receptors in stress-induced relapse to cocaine seeking behaviour. Biochem Pharmacol 83: 1–5.

Hague C, Chen Z, Pupo AS, Schulte NA, Toews ML, Minneman KP (2004a). The N terminus of the human alpha1D-adrenergic receptor prevents cell surface expression. J Pharmacol Exp Ther 309: 388–397.

Hague C, Uberti MA, Chen Z, Hall RA, Minneman KP (2004b). Cell surface expression of alpha1D-adrenergic receptors is controlled by heterodimerization with alpha1B-adrenergic receptors. J Biol Chem 279: 15541–15549.

Hahn J, Hopf FW, Bonci A (2009). Chronic cocaine enhances corticotropin-releasing factor-dependent potentiation of excitatory transmission in ventral tegmental area dopamine neurons. J Neurosci 29: 6535–6544.

Hasbi A, Fan T, Alijaniaram M, Nguyen T, Perreault ML, O'Dowd BF *et al.* (2009). Calcium signaling cascade links dopamine D1–D2 receptor heteromer to striatal BDNF production and neuronal growth. Proc Natl Acad Sci U S A 106: 21377–21382.

Hasbi A, O'Dowd BF, George SR (2010). Heteromerization of dopamine D2 receptors with dopamine D1 or D5 receptors generates intracellular calcium signaling by different mechanisms. Curr Opin Pharmacol 10: 93–99.

Heckman KL, Pease LR (2007). Gene splicing and mutagenesis by PCR-driven overlap extension. Nat Protoc 2: 924–932.

Juhasz JR, Hasbi A, Rashid AJ, So CH, George SR, O'Dowd BF (2008). Mu-opioid receptor heterooligomer formation with the dopamine D1 receptor as directly visualized in living cells. Eur J Pharmacol 581: 235–243.

Kaupmann K, Malitschek B, Schuler V, Heid J, Froestl W, Beck P *et al.* (1998). GABA(B)-receptor subtypes assemble into functional heteromeric complexes. Nature 396: 683–687.

Koob GF (2008). A role for brain stress systems in addiction. Neuron 59: 11–34.

Lee SP, So CH, Rashid AJ, Varghese G, Cheng R, Lanca AJ *et al.* (2004). Dopamine D1 and D2 receptor Co-activation generates a novel phospholipase C-mediated calcium signal. J Biol Chem 279: 35671–35678.

Leyton V, Goles NI, Fuenzalida-Uribe N, Campusano JM (2014). Octopamine and dopamine differentially modulate the

nicotine-induced calcium response in *Drosophila* mushroom body Kenyon cells. Neurosci Lett 560: 16–20.

Liu J, Yu B, Orozco-Cabal L, Grigoriadis DE, Rivier J, Vale WW *et al.* (2005). Chronic cocaine administration switches corticotropin-releasing factor2 receptor-mediated depression to facilitation of glutamatergic transmission in the lateral septum. J Neurosci 25: 577–583.

Lovenberg TW, Chalmers DT, Liu C, De Souza EB (1995). CRF2 alpha and CRF2 beta receptor mRNAs are differentially distributed between the rat central nervous system and peripheral tissues. Endocrinology 136: 4139–4142.

Lukkes JL, Staub DR, Dietrich A, Truitt W, Neufeld-Cohen A, Chen A *et al.* (2011). Topographical distribution of corticotropin-releasing factor type 2 receptor-like immunoreactivity in the rat dorsal raphe nucleus: co-localization with tryptophan hydroxylase. Neuroscience 183: 47–63.

Magalhaes AC, Holmes KD, Dale LB, Comps-Agrar L, Lee D, Yadav PN *et al.* (2010). CRF receptor 1 regulates anxiety behavior via sensitization of 5-HT2 receptor signaling. Nat Neurosci 13: 622–629.

Margeta-Mitrovic M, Jan YN, Jan LY (2000). A trafficking checkpoint controls GABA(B) receptor heterodimerization. Neuron 27: 97–106.

Markovic D, Punn A, Lehnert H, Grammatopoulos DK (2008). Intracellular mechanisms regulating corticotropin-releasing hormone receptor-2beta endocytosis and interaction with extracellularly regulated kinase 1/2 and p38 mitogen-activated protein kinase signaling cascades. Mol Endocrinol 22: 689–706.

Mellado M, Rodriguez-Frade JM, Vila-Coro AJ, Fernandez S, Martin de Ana A, Jones DR *et al.* (2001). Chemokine receptor homo- or heterodimerization activates distinct signaling pathways. EMBO J 20: 2497–2507.

Neve KA, Seamans JK, Trantham-Davidson H (2004). Dopamine receptor signaling. J Recept Signal Transduct Res 24: 165–205.

O'Dowd BF, Ji X, Alijaniaram M, Rajaram RD, Kong MM, Rashid A *et al.* (2005). Dopamine receptor oligomerization visualized in living cells. J Biol Chem 280: 37225–37235.

Orozco-Cabal L, Liu J, Pollandt S, Schmidt K, Shinnick-Gallagher P, Gallagher JP (2008). Dopamine and corticotropin-releasing factor synergistically alter basolateral amygdala-to-medial prefrontal cortex synaptic transmission: functional switch after chronic cocaine administration. J Neurosci 28: 529–542.

Pawson AJ, Sharman JL, Benson HE, Faccenda E, Alexander SP, Buneman OP *et al.*; NC-IUPHAR (2014). The IUPHAR/BPS Guide to PHARMACOLOGY: an expert-driven knowledgebase of drug targets and their ligands. Nucl. Acids Res. 42 (Database Issue): D1098–106.

Perreault ML, Hasbi A, O'Dowd BF, George SR (2014). Heteromeric dopamine receptor signaling complexes: emerging neurobiology and disease relevance. Neuropsychopharmacology 39: 156–168.

Rashid AJ, So CH, Kong MM, Furtak T, El-Ghundi M, Cheng R *et al.* (2007). D1-D2 dopamine receptor heterooligomers with unique pharmacology are coupled to rapid activation of Gq/11 in the striatum. Proc Natl Acad Sci U S A 104: 654–659.

Rutz C, Renner A, Alken M, Schulz K, Beyermann M, Wiesner B *et al.* (2006). The corticotropin-releasing factor receptor type 2a contains an N-terminal pseudo signal peptide. J Biol Chem 281: 24910–24921.

Saal D, Dong Y, Bonci A, Malenka RC (2003). Drugs of abuse and stress trigger a common synaptic adaptation in dopamine neurons. Neuron 37: 577–582.

Schulz K, Rutz C, Westendorf C, Ridelis I, Vogelbein S, Furkert J *et al.* (2010). The pseudo signal peptide of the corticotropin-releasing factor receptor type 2a decreases receptor expression and prevents Gi-mediated inhibition of adenylyl cyclase activity. J Biol Chem 285: 32878–32887.

Shalev U, Erb S, Shaham Y (2010). Role of CRF and other neuropeptides in stress-induced reinstatement of drug seeking. Brain Res 1314: 15–28.

So CH, Varghese G, Curley KJ, Kong MM, Alijaniaram M, Ji X *et al.* (2005). D1 and D2 dopamine receptors form heterooligomers and cointernalize after selective activation of either receptor. Mol Pharmacol 68: 568–578.

Sun P, Wang J, Gu W, Cheng W, Jin GZ, Friedman E *et al.* (2009). PSD-95 regulates D1 dopamine receptor resensitization, but not receptor-mediated Gs-protein activation. Cell Res 19: 612–624.

Teichmann A, Rutz C, Kreuchwig A, Krause G, Wiesner B, Schulein R (2012). The Pseudo signal peptide of the corticotropin-releasing factor receptor type 2A prevents receptor oligomerization. J Biol Chem 287: 27265–27274.

Terrillon S, Bouvier M (2004). Roles of G-protein-coupled receptor dimerization. EMBO Rep 5: 30–34.

Verma V, Hasbi A, O'Dowd BF, George SR (2010). Dopamine D1-D2 receptor heteromer-mediated calcium release is desensitized by D1 receptor occupancy with or without signal activation: dual functional regulation by G protein-coupled receptor kinase 2. J Biol Chem 285: 35092–35103.

Vickery RG, von Zastrow M (1999). Distinct dynamin-dependent and -independent mechanisms target structurally homologous dopamine receptors to different endocytic membranes. J Cell Biol 144: 31–43.

Vilardaga JP, Nikolaev VO, Lorenz K, Ferrandon S, Zhuang Z, Lohse MJ (2008). Conformational cross-talk between alpha2A-adrenergic and mu-opioid receptors controls cell signaling. Nat Chem Biol 4: 126–131.

Wang B, Shaham Y, Zitzman D, Azari S, Wise RA, You ZB (2005). Cocaine experience establishes control of midbrain glutamate and dopamine by corticotropin-releasing factor: a role in stress-induced relapse to drug seeking. J Neurosci 25: 5389–5396.

Wang B, You ZB, Rice KC, Wise RA (2007). Stress-induced relapse to cocaine seeking: roles for the CRF(2) receptor and CRF-binding protein in the ventral tegmental area of the rat. Psychopharmacology (Berl) 193: 283–294.

Waselus M, Nazzaro C, Valentino RJ, Van Bockstaele EJ (2009). Stress-induced redistribution of corticotropin-releasing factor receptor subtypes in the dorsal raphe nucleus. Biol Psychiatry 66: 76–83.

Zorrilla EP, Logrip ML, Koob GF (2014). Corticotropin releasing factor: a key role in the neurobiology of addiction. Front Neuroendocrinol 35: 234–244.